ELSEVIER

Materials Science and Engineering A 435–436 (2006) 412–417

MATERIALS SCIENCE & ENGINEERING A

www.elsevier.com/locate/msea

Tension–tension fatigue damage characteristics of a 3D SiC/SiC composite in H_2O–O_2–Ar environment at 1300 °C

Shoujun Wu *, Laifei Cheng, Jun Zhang, Litong Zhang, Xingang Luan, Hui Mei, Peng Fang

National Key Laboratory of Thermostructure Composite Materials, Northwestern Polytechnical University, Xi'an Shaanxi 710072, People's Republic of China

Received 27 May 2006; received in revised form 5 July 2006; accepted 14 July 2006

Abstract

Tension–tension fatigue behaviors of a 3D woven SiC fiber (Hi-Nicalon) reinforced CVI SiC–matrix composite were measured in a H_2O–O_2–Ar environment at 1300 °C. The results indicated that the SiC/SiC had excellent fatigue resistance in H_2O–O_2–Ar atmosphere. Fiber/matrix interface debonding, sliding and fibers pull out in tension–tension fatigue tests were more obvious than those in monotonic tension tests. The cross-section surface of the monotonic tension specimens was coarse in whole, while that of the fatigue specimens were composed of ringed striations and smooth area. During tension–tension fatigue test, the coexisting damage characteristics were: (i) cracking of SiC matrix, disengaging of SiC matrix and grains growth; (ii) partial oxidation or burn out of pyrolytic carbon (PyC) interlayer and severe oxidation of fibers; (iii) fibers torn and fracture.

Keywords: SiC/SiC composite; Tension–tension fatigue; Oxidation; Water vapor; Damage

1. Introduction

Silicon carbide fiber reinforced SiC–matrix composites fabricated by chemical vapor infiltration (CVI) process (SiC/SiC) have been intensively researched as one of the most promising thermal structural materials due to their high toughness, good resistance to thermal shock, good mechanical properties at high temperature, especially improved flaw tolerance and noncatastrophic mode of failure [1–4]. As an example, SiC/SiC can be used as combustor liners and turbine vanes for propulsion power generation.

In many cases, high-loading frequency and temperature capabilities are required when SiC/SiC was used as some components in reusable launch vehicles and/or space applications. One of such applications is its use in a CMC bladed disk for rocket engine turbopumps [5]. Moreover, in combustion process, substantial amounts of water vapor are produced from burning hydrocarbon fuels in air. Calculations showed that 5–10% of the combustion gas is water vapor under equilibrium conditions [6]. Therefore, the knowledge on fatigue behaviors of this kind of materials in the moisture environment at elevated temperature is important to their applications in harsh environments.

The fatigue behaviors of SiC/SiC composites have been researched [7–13]. It should be noted that: firstly, the reinforcements involved are mainly 2D woven SiC cloth which contain a relative higher content of oxygen (14.4 or 15 wt.%) [7–9] and the research interesting were focused on damage characterization by the effective dynamic modulus of elasticity and the corresponding damping coefficient [8,9]. Secondly, some of the involved composites contained boron [8,10,11] which had distinct effects on the oxidation behavior [14], especially in wet oxidizing environment. Thirdly, few researches were conducted in wet environment [11], and the experimental temperature was much lower than the application environment. Hi-Nicalon fiber is oxygen-free fibers consisting of a mixture of SiC-nanocrystals (≈5 nm in mean size) and free carbon [C/Si (at.) ratio = 1.39]. It is well known that the thermo-mechanical properties of fiber reinforced composites was greatly influenced by the architecture of fiber preforms, especially chemical composition, microstructure of fibers and its strength as well as the service environments [1,15–17]. Thus, the fatigue behavior of the Hi-Nicalon fiber reinforced CVI SiC–matrix composites may be different form the reported ones. However, up to now, the research on the fatigue damage characteristics of SiC/SiC, especially the research results of Hi-Nicalon fiber reinforced CVI SiC–matrix

* Corresponding author. Tel.: +86 29 8848 6068 828; fax: +86 29 8849 4620.
E-mail address: shoujun_wu@163.com (S. Wu).

0921-5093/$ – see front matter © 2006 Elsevier B.V. All rights reserved.
doi:10.1016/j.msea.2006.07.041

composite fabricated by four-step three-dimensional (4-step 3D) in water-containing environment have not been found.

The present investigation presents the tension–tension fatigue damage behaviors of a 3D PyC-interphase SiC/SiC composite (reinforced by Hi-Nicalon SiC fibers) with a CVD SiC coating in a H_2O–O_2–Ar environments at 1300 °C. Much of analysis and discussion will then focus on the fatigue characteristics of the composite.

2. Materials and experimental procedure

2.1. Sample preparation

SiC fiber (Hi-Nicalon, Nippon Carbon Co., Japan) preform was prepared using four-step three-dimensional (4-step 3D) braiding method. Low pressure chemical vapor infiltration (LPCVI) process was employed to deposit pyrolytic carbon (PyC) as an interphase and silicon carbide as a matrix. The volume fraction of SiC fiber was about 40% and the braiding angle was about 20°. PyC layer was deposited on the fiber by decompositions of C_3H_6 at 870 °C for 1 h at reduced pressure of 5 kPa in a CVI reactor, arriving to a thickness of 0.2 μm. Methyltrichlorosilane (MTS, CH_3SiCl_3) was used for the deposition of SiC, carried by bubbling hydrogen in gas phase and argon as the dilute gas to slow down the chemical reaction rate during deposition. SiC matrix was prepared at 1100 °C for 120 h (30 h per times) at reduced pressure of 5 kPa, and the molar ratio of H_2 to MTS was 10. The as-received SiC/SiC was cut into dog-bone samples (showed in Fig. 1) along the fibers longitudinal direction. Density and open porosity of the samples were 2.7 g cm^{-3} and 7.3%, respectively, measured by Archimedes method. A CVD SiC coating was deposited on the samples for 20 h to seal the open ends of the fibers.

2.2. Test details

The monotonic tensile tests were performed at room temperature to determine the tensile properties of the material, namely, the ultimate tensile stress and to compare the damage characteristics. The load increased at a constant rate of 0.001 mm s^{-1} up to fracture of the specimens. The displacement, load and strain were monitored.

Tension–tension fatigue tests of the SiC/SiC composite were conducted in a H_2O–O_2–Ar environment at 1300 °C. Tension–tension fatigue tests were conducted with integrated system including a resistance heating furnace and a servo-hydraulic machine (Model INSTRON 8801 from INSTRON Ltd., England). Only the gauge parts of the specimens (40 mm long, 3 mm wide and 3 mm thick) were kept in the hot zone and oxidizing atmospheres. Deionized water was used to engender water vapor. The partial pressure of water vapor, oxygen and argon was 15, 8 and 78 kPa, respectively. The flux of gases was accurately controlled by a mass flow controller (5850 i series from BROOKS, in Japan) with a precision of 0.1 SCCM. The tests were run under a maximum applied stress of 120 MPa, at a frequency of 1 Hz and with a stress ratio of $R = 0.5$ ($R = \sigma_{min}/\sigma_{max}$), with a sinusoidal wave form. In order to gain knowledge of the tension–tension fatigue life of the SiC/SiC in H_2O–O_2–Ar environment, the tests were carried out until the specimen fully failed.

Microstructures of the samples before and after tests were examined using a scanning electron microscope (SEM, S4700).

3. Results

3.1. Monotonic tensile behavior of the SiC/SiC composite

The average ultimate tensile strength (UTS) of the SiC/SiC composites at room temperature measured from the monotonic tension test was 456 ± 40 MPa.

Fig. 2 shows the typical load–extension curve of the SiC/SiC measured under monotonic tension at room temperature. The load–extension curve indicated initially a linear elastic behavior up to the proportional limit of 1000 N (corresponding to about 130 MPa), which was about 29% of the ultimate tensile strength. Then the curve showed a continuously decreasing slope and associated non-linear displacements. After that, the curve showed a linear portion till the fracture of the composite. It should be noted that the load–extension curve for all specimens showed a slight steep drop in the final portion at the load range from 2500 to 2800 N (326–365 MPa), then the curve quickly restored. This monotonic tensile curve of the 4-step 3D SiC/SiC in this study is different from those observed in 2D SiC/SiC and those in 3D SiC/SiC with an orthogonal architecture [11,18].

It has been supposed that the linear proportion in load–extension curve represents the portion before any appreciable amount of matrix crack, developed in the composite [11]. The non-linear in curve or the transition was due to the sub-

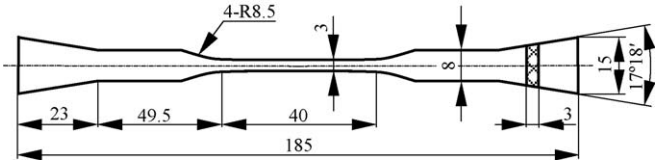

Fig. 1. A schematic showing of the dog-bone shape SiC/SiC specimen (the unit was mm).

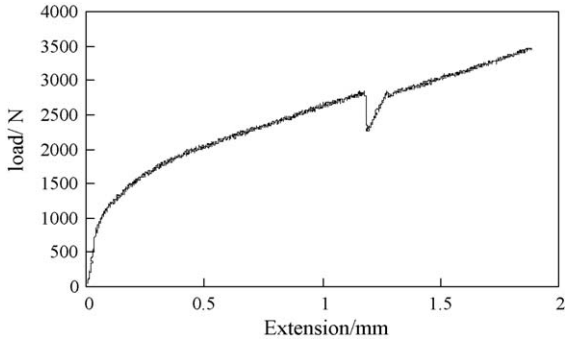

Fig. 2. Typical load–extension curves of the 3D SiC/SiC composite in monotonic tension at room temperature.

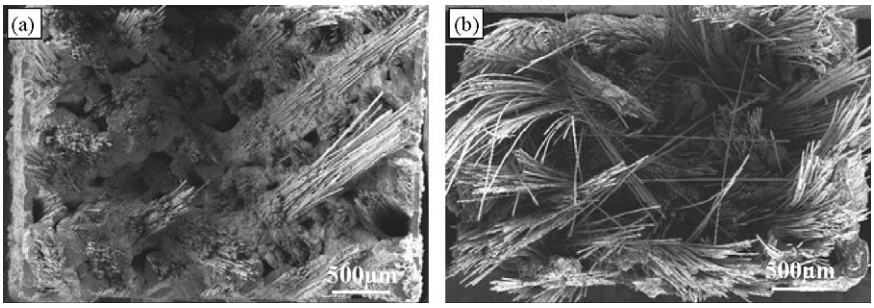

Fig. 3. Cross-section morphologies of the 3D SiC/SiC composite after: (a) monotonic tension test; (b) tension–tension fatigue test.

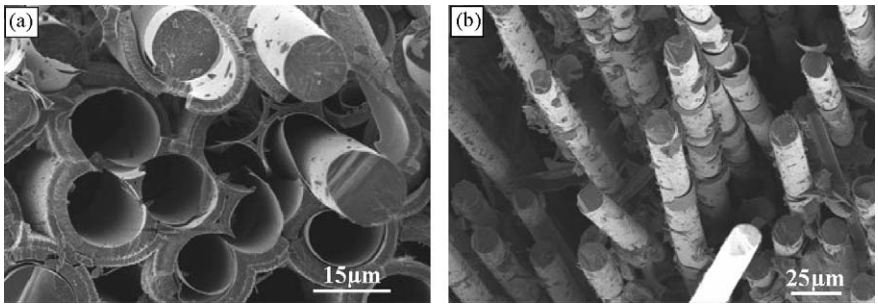

Fig. 4. (a) Fiber/matrix interface debonding; (b) fibers sliding and pull out in the SiC/SiC composite after tension–tension fatigue.

sequent matrix/fiber interface debonding and sliding of fibers. The final linear portion was mainly owing to the damage regime [19]. At this study, due to the fibers preform was prepared by 4-step 3D method, the braiding angle may be reduced when the matrix damaged under the tension load. Consequently, the slight steep drop in the final linear portion is supposed to come from the reduction of this braiding angle.

3.2. Tension–tension fatigue damage characteristics

Tension–tension fatigue of the 3D SiC/SiC composite in the H_2O–O_2–Ar environments at 1300 °C lasted up to 105 h and 12 min indicating the composite has excellent fatigue capacity. However, the damage characteristics should be clarified, because it is important to design, evaluate and maintain the components made of this SiC/SiC composite in engines application. In this part, damage characteristics after the tension–tension fatigue tests were reported.

Fig. 3 shows the cross-section of the specimens after monotonic tension test and tension–tension fatigue tests. The fibers pull out in tension–tension fatigue tested specimens was more and longer than that in monotonic tested specimens. Moreover, the fibers in tension–tension fatigue tested specimens were much looser, while those in monotonic tested specimens kept bunchiness. These results indicate that fiber/matrix interface debonding, sliding and fibers pull out in tension–tension fatigue tests were more obvious than those in monotonic tension tests, as shown in Fig. 4.

Fig. 5 shows the comparison of cross-section morphologies of fibers in the SiC/SiC composite after tension–tension fatigue test and after monotonic tension test, respectively. It shows that the whole cross-section surface of the monotonic tension tested specimens was coarse. However, the cross-section surface of the tension–tension fatigue tested specimens can be obviously divided into two different areas: one area was composed of ringed striations which took up about half of the whole section, while the other area was smooth.

Fig. 6 shows the micromorphologies of SiC matrix in the SiC/SiC after tension–tension fatigue test. It can be seen that three changes occurred in the matrix. Firstly, the matrix cracked

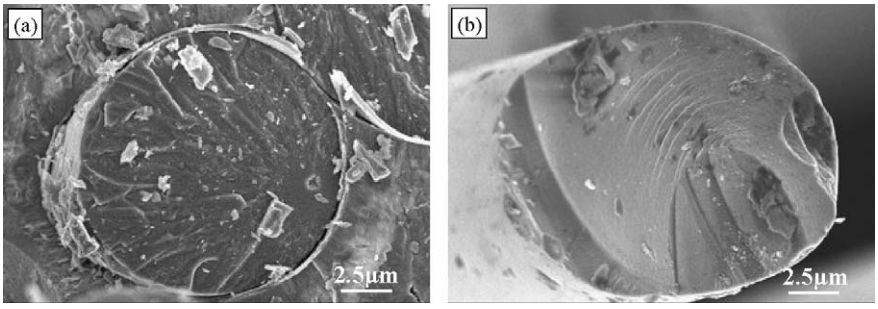

Fig. 5. Cross-section morphologies of the fibers in 3D SiC/SiC composite after: (a) monotonic tension test; (b) tension–tension fatigue test.

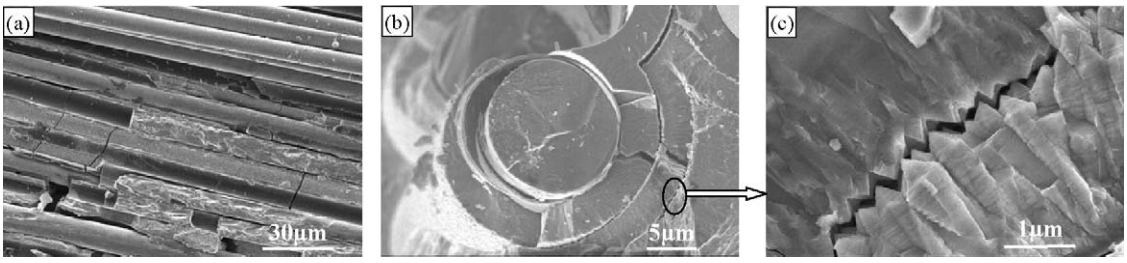

Fig. 6. (a) Cracking of SiC matrix; (b and c) disengaging of SiC matrix and grains growth in the 3D SiC/SiC composite after tension–tension fatigue.

perpendicularly to longitudinal direction of fiber bundles as shown in Fig. 6(a). Secondly, the SiC matrix zigzag delamination at interface of two depositions, as shown in Fig. 6(b and c). Thirdly, the SiC grains evidently grow up, as shown in Fig. 6(c).

4. Discussion

During monotonic loading, the fibers were first undamaged, then the volume fraction of broken fibers also increased leading to the sliding areas at the fiber/matrix interface. Hence, the failure behavior of ceramic–matrix composites depends mainly on two microstructural parameters: (i) the individual failure stress distribution of the fibers and (ii) the characteristics of the fiber/matrix interface. In fiber reinforced CVI matrix composite, the fiber bundles were tightly constrained by CVI matrix, acting as a unitary unit under load. As shown in Fig. 7, the PyC interphase was closely bonded to both CVI SiC matrix and Hi-Nicalon fiber. Therefore, it was difficult for the Hi-Nicalon SiC fiber to debond and to be pulled out from the silicon carbide matrix, which resulted in the fracture of fibers was mainly in bundles. Though the stress was much lower for matrix cracking or the composite fracture during tension–tension fatigue load, it resulted in the braiding architecture of the composite changed, i.e. braiding angle reduction due to the repeat loading. The braiding angle reduction led to microcracks propagation and reduction of constrains between matrix and fibers, which result in the cracking of the SiC matrix at the interface of two depositions. Thus, the 3D SiC/SiC composite after tension–tension fatigue tests showed a more obvious pull out than that in monotonic tension tests. Furthermore, the deposited SiC-nanogranules [20] grew under the cooperation of stress inducement [21,22] and long time exposure at high temperature.

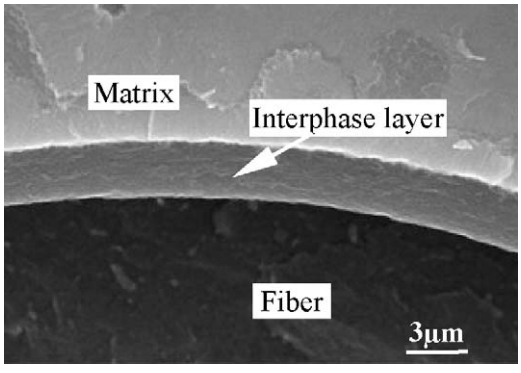

Fig. 7. Typical micromorphology of fiber/interphase/matrix in the as-received 3D SiC/SiC composite.

The cracking of matrix resulted in the diffusion of oxidizing gas, namely oxygen and water vapor, into the PyC interlayer, which led to oxidation of PyC and SiC phases at 1300 °C in two possible manners: (1) the opening width of microcracks was much narrow and the amount of oxygen was few for burning out of PyC before the specimens fractured. In this case, oxidation consumption of PyC interlayer was predominant and the oxidation of the SiC phase was rather less as shown in Fig. 8(a), which was favorable to subsequent oxidation and fibers pull out. (2) The microcracks were relatively wider than the former, the amount of oxygen was too much for the burn out of PyC before specimens fractured. In this case, the SiC phase was severely oxidized, as shown in Fig. 8(b–e), so that the fibers and matrix adhered to each other by the formed SiO_2 as shown in Fig. 8(b). Thus, the sliding and pull out of fibers will be hampered by the adhesion of SiO_2. As a result, due to adhesion between fiber and matrix by the formed SiO_2, some of the fibers will be unilaterally torn during pull out under tensile load, as shown in Fig. 8(f). It is obviously that all of these different types of damage characteristics were coexistent. On the other hand, the formed SiO_2 may crack during the change of tension load.

As shown in Fig. 9, when the specimen was under tensile load, the tensile stress in fibers flexural outboard was higher than that in inboard because the fibers were tortuous. Under tension–tension fatigue, when the load is higher than average value, microcracks on the fibers' outboard surface will extend in radial direction. When the load was below average level, the stress in the whole fiber might be released and there were no microcracks propagation occurred. Consequently, the microcracks propagation is off and on when the specimens are loaded fluctuating tensile load which led to the fiber shows ringed striations. When the microcracks propagated to where is the center of fibers, it is supposed that the fibers will suddenly brittle fractured due to stress concentration and the effective stress was much higher than tensile strength. Thus, the cross-section surface of fibers showed a smooth area as a result of brittle fracture of fibers.

Furthermore, it can be concluded that these damage characteristics of 4-step 3D SiC/SiC composite in tension–tension fatigue was directly related to the braiding architecture of fiber preform, which determined the characteristics of stress state, matrix changes and fibers damage and pull out.

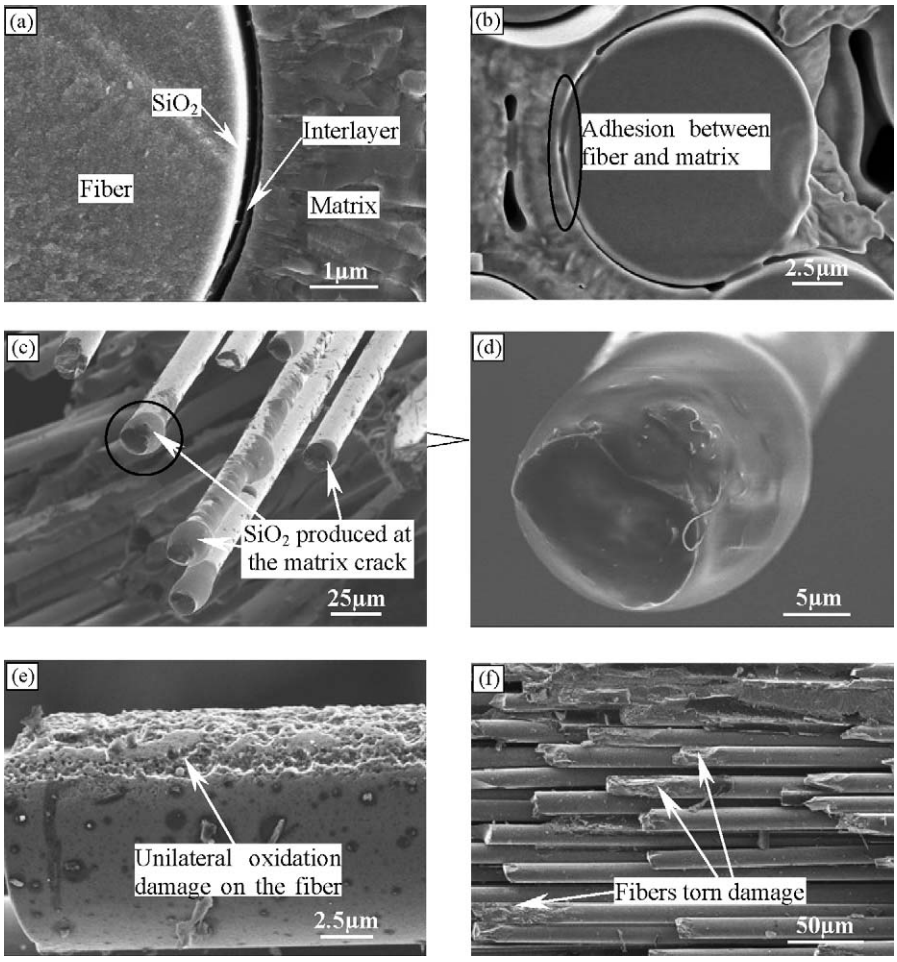

Fig. 8. Different types of oxidation and fibers damage in the SiC/SiC composite after tension–tension fatigue in wet oxidizing environments at 1300 °C for 105 h and 12 min: (a) partial oxidation of PyC interlayer; (b) adhesion between fibers and matrix; (c) SiO_2 locally formed at the matrix cracks; (d) magnified view of (c); (e) unilateral oxidation damage on the fiber surface; (f) fibers torn damage.

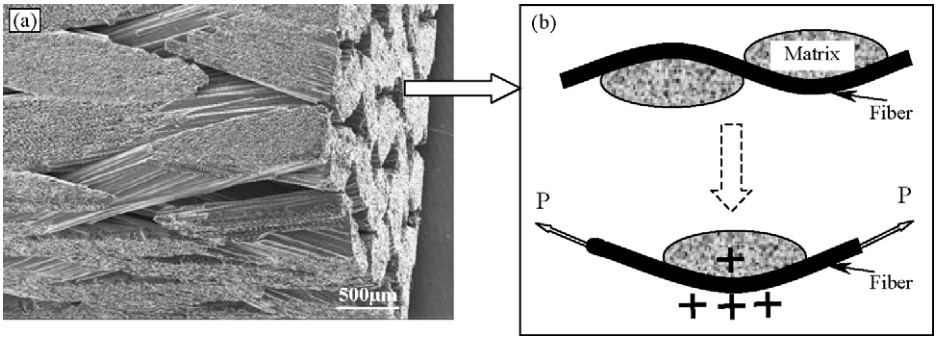

Fig. 9. (a) SEM image of the fibers preform fabricated by 4-step 3D braiding method; (b) schematic of stress state of the fibers and matrix under tensile load.

5. Conclusions

A three-dimensional SiC/SiC composite was prepared by chemical vapor infiltration process, and tension–tension fatigue test of the SiC/SiC composite was carried out in a H_2O–O_2–Ar environment at 1300 °C. The results indicated that the SiC/SiC has excellent fatigue capacity as the tests lasted up to 105 h and 12 min.

Fiber/matrix interface debonding, sliding and fibers pull out in tension–tension fatigue tests were more obvious than those in monotonic tension tests. The fracture surface of the monotonic tension specimens was coarse while that of the fatigue specimens shows two different areas, namely ringed striations and smooth area. During tension–tension fatigue, the coexisting damage characteristics were: (i) cracking of SiC matrix, disengaging of SiC matrix and grains growth; (ii) PyC interlayer

partial oxidation or burn out and fibers severe oxidation due to diffusion of oxidizing gas through the matrix cracks; (iii) fibers torn and fracture.

Tension–tension fatigue damage characteristics of fiber reinforced composite were directly affected by braiding architecture of the fibers preform.

Acknowledgements

The authors acknowledge the support of the Chinese National Foundation for Natural Sciences under Contract No. 90405015, the NSFC Distinguished Young Scholar under Contract No. 50425208 (2004), the program for Changjiang Scholars and Innovative Research Team in University.

References

[1] R. Naslain, Compos. Sci. Technol. 64 (2004) 155–170.
[2] S. Schmidt, S. Beyer, H. Knabe, et al., Acta Astronaut. 55 (2004) 409–420.
[3] J. Kimmel, N. Miriyala, J. Price, K. More, et al., J. Eur. Ceram. Soc. 22 (2002) 2769–2775.
[4] C.G. Papakonstantinou, P. Balaguru, R.E. Lyon, Compos. Part B Eng. 32 (2001) 637–649.
[5] M.R. Effinger, G.G. Genge, J.D. Kiser, Adv. Mater. Process. 157 (2000) 69–73.
[6] N.S. Jacobson, J. Am. Ceram. Soc. 76 (1993) 3–28.
[7] S. Pasquier, J. Lamon, R. Naslain, Compos. Part A Appl. 29 (1998) 1157–1164.
[8] M. Mizuno, S.J. Zhu, Y. Kagawa, H. Kaya, J. Eur. Ceram. Soc. 18 (1998) 1869–1878.
[9] V. Kostopoulos, Y.Z. Pappas, Y.P. Markopoulos, J. Eur. Ceram. Soc. 19 (1999) 207–215.
[10] S. Zhu, M. Mizuno, Y. Kagawa, Y. Mutoh, Compos. Sci. Technol. 59 (1999) 833–851.
[11] S. Mall, Mater. Sci. Eng. A 412 (2005) 165–170.
[12] P. Reynaud, Compos. Sci. Technol. 56 (1996) 809–814.
[13] Y. Miyashita, K. Kanda, S. Zhu, Y. Mutoh, M. Mizuno, A.J. McEvily, Int. J. Fatigue 24 (2002) 241–248.
[14] J. Schlichting, High Temp.-High Press. 14 (1982) 717–724.
[15] H. Ichikawa, Ann. Chim. Sci. Mater. 25 (2000) 523–528.
[16] M. Takeda, J. Sakamoto, Y. Imai, H. Ichikawa, Compos. Sci. Technol. 59 (1999) 813–819.
[17] M. Takeda, A. Urano, J. Sakamoto, Y. Imai, J. Nucl. Mater. 258–263 (1998) 1594–1599.
[18] P. Lipetzky, G.J. Dvorak, N.S. Stoloff, Mater. Sci. Eng. A 216 (1996) 11–19.
[19] D. Beyerley, S.M. Spearing, F.W. Zok, A.G. Evans, J. Am. Ceram. Soc. 75 (1992) 2719–2725.
[20] Y.D. Xu, L.F. Cheng, L.T. Zhang, J. Mater. Process. Technol. 101 (2000) 47–51.
[21] A.J. Haslam, D. Moldovan, V. Yamakov, D. Wolf, S.R. Phillpot, H. Gleiter, Acta Mater. 51 (2003) 2097–2112.
[22] F.R.N. Nabarro, Scripta Mater. 39 (1998) 1681–1683.